Molecular and Cellular Biology

Extracellular pH Dynamically Controls Cell Surface Delivery of Functional TRPV5 Channels

Tim T. Lambers, Elena Oancea, Theun de Groot, Catalin N. Topala, Joost G. Hoenderop and René J. Bindels
Mol. Cell. Biol. **2007, 27(4):1486. DOI: 10.1128/MCB.01468-06.**
Published Ahead of Print 18 December 2006.

MOLECULAR AND CELLULAR BIOLOGY, Feb. 2007, p. 1486–1494 Vol. 27, No. 4
0270-7306/07/$08.00+0 doi:10.1128/MCB.01468-06

Extracellular pH Dynamically Controls Cell Surface Delivery of Functional TRPV5 Channels▽

Tim T. Lambers,[1] Elena Oancea,[2] Theun de Groot,[1] Catalin N. Topala,[1] Joost G. Hoenderop,[1] and René J. Bindels[1]*

Department of Physiology, Nijmegen Centre for Molecular Life Sciences, Radboud University Nijmegen Medical Centre, Nijmegen, The Netherlands,[1] and Department of Cardiology, Howard Hughes Medical Institute, Children's Hospital Boston, Harvard Medical School, Boston, Massachusetts[2]

Received 8 August 2006/Returned for modification 18 September 2006/Accepted 2 December 2006

Extracellular pH has long been known to affect the rate and magnitude of ion transport processes among others via regulation of ion channel activity. The Ca^{2+}-selective transient receptor potential vanilloid 5 (TRPV5) channel constitutes the apical entry gate in Ca^{2+}-transporting cells, contributing significantly to the overall Ca^{2+} balance. Here, we demonstrate that extracellular pH determines the cell surface expression of TRPV5 via a unique mechanism. By a comprehensive approach using total internal reflection fluorescence microscopy, cell surface protein labeling, electrophysiology, $^{45}Ca^{2+}$ uptake assays, and functional channel recovery after chemobleaching, this study shows that upon extracellular alkalinization, a pool of TRPV5-containing vesicles is rapidly recruited to the cell surface without collapsing into the plasma membrane. These vesicles contain functional TRPV5 channels since extracellular alkalinization is accompanied by increased TRPV5 activity. Conversely, upon subsequent extracellular acidification, vesicles are retrieved from the plasma membrane, simultaneously resulting in decreased TRPV5 activity. Thus, TRPV5 accesses the extracellular compartment via transient openings of vesicles, suggesting that rapid responses of constitutive active TRP channels to physiological stimuli rely on vesicular "kiss and linger" interactions with the plasma membrane.

The superfamily of transient receptor potential (TRP) channels is involved in diverse physiological processes, ranging from sensory activity to fertility and epithelial ion transport (15). The highly Ca^{2+}-selective TRP vanilloid 5 (TRPV5) channel constitutes the apical entry gate in Ca^{2+}-transporting cells and facilitates renal Ca^{2+} influx from the prourine (10). Several lines of evidence indicate that TRPV5 activity is sensitive to pH. First, acid-based homeostasis is known to affect renal Ca^{2+} handling as reflected by altered Ca^{2+} excretion in kidneys during chronic acidosis or alkalosis, which is mediated at least in part by changes in TRPV5 gene expression (16). Second, in vitro studies indicated that intra- and extracellular pH directly regulate the activity of TRPV5. Acidification inhibited, whereas alkalinization stimulated, TRPV5 activity, likely mediated by conformational changes of the channel pore helix (24–26).

An intrinsic physiological effect of extracellular pH is the regulation of trafficking processes like endo- and exocytosis and lysosomal trafficking (8, 12, 14). Since several TRP channels display constitutive activity, controlled recruitment of these channels towards the plasma membrane is important for the translation of physiological stimuli into increased ion permeability of the plasma membrane. For instance, an essential process during insulin-like growth factor-I stimulation of cell growth is TRPV2 recruitment facilitating Ca^{2+} entry during progression through the cell cycle (11). In *Drosophila* photoreceptors, the TRP-like subunit is shuttled between the plasma membrane and an intracellular compartment by a light-regulated mechanism to fine-tune visual responses (1). Furthermore, the rapid insertion of TRPC5 channels into the plasma membrane was recently identified as a mechanism underlying epidermal growth factor (EGF)-hormone-induced neurite extension in cultured hippocampal neurons (2). However, rapid plasma membrane recruitment of TRPV5 by extracellular physiological stimuli to control its activity in Ca^{2+}-transporting epithelia has not been studied.

The aim of the present study was to investigate the effect of extracellular pH on TRPV5 plasma membrane recruitment as a mechanism underlying pH-dependent channel activity. By using total internal reflection fluorescence (TIRF) microscopy, cell surface protein labeling, electrophysiology, $^{45}Ca^{2+}$ uptake assays, and functional recovery after chemobleaching (FRAC), this study revealed that plasma membrane expression of TRPV5 is under the control of extracellular pH and relies on TRPV5-containing vesicles which fuse but do not collapse during recruitment and subsequent retrieval. Our results contribute to the concept of "kiss and linger" delivery of constitutive active TRP channels in response to physiological stimuli.

* Corresponding author. Mailing address: 286 Physiology, Nijmegen Centre for Molecular Life Sciences, Radboud University Nijmegen Medical Centre, P.O. Box 9101, 6500 HB Nijmegen, The Netherlands. Phone: 31 24 3614211. Fax: 31 24 3616413. E-mail: R.Bindels@ncmls.ru.nl.

▽ Published ahead of print on 18 December 2006.

MATERIALS AND METHODS

Molecular biology and cell culture. pCINEO/IRES-GFP-HA-TRPV5, pCINEO/IRES-GFP, EGFP-TRPV5, and EGFP-TRPM7 were constructed and transiently transfected in HEK293T cells as described previously (5, 17). Madin-Darby canine

kidney type-I epithelial (MDCK) cells were stably transfected with EGFP-TRPV5 as described previously (5).

$^{45}Ca^{2+}$ uptake assay and electrophysiology. $^{45}Ca^{2+}$ uptake was determined using EGFP-, EGFP-TRPM7-, and EGFP-TRPV5-transfected HEK293T cells and confluent layers of MDCK cells stably expressing EGFP-TRPV5. After 10 min of incubation in KHB buffer (for TRPV5, 110 mM NaCl, 5 mM KCl, 1.2 mM $MgCl_2$, 0.1 mM $CaCl_2$, 10 mM Na-acetate, 2 mM NaH_2PO_4, and 20 mM HEPES, pH 6.0, 7.4, or 8.5, with HCl/NaOH; for TRPM7, 110 mM NaCl, 5 mM KCl, 10 mM Na-acetate, and 20 mM HEPES, pH 6.0, 7.4, or 8.5, with HCl/NaOH), cells were incubated for 6 to 10 min with $^{45}CaCl_2$ (1 μCi/ml) in KHB buffer with 4 mM L-lactate, 10 mM D-glucose, 1 mM L-alanine, and voltage-gated Ca^{2+} channel inhibitors (10 μM felodipine and 10 μM verapamil). Cells were incubated with 10 μM ruthenium red to block TRPV5-mediated $^{45}Ca^{2+}$ uptake. After washing with ice-cold stop buffer (110 mM NaCl, 5 mM KCl, 1.2 mM $MgCl_2$, 10 mM Na-acetate, 20 mM HEPES, 0.5 mM $CaCl_2$, and 1.5 mM $LaCl_3$, pH 6.0, 7.4, or 8.5), $^{45}Ca^{2+}$ uptake was measured. Whole-cell currents of HEK293 cells transiently transfected with pCINEO/IRES-GFP-HA-TRPV5 or the corresponding E522Q and K607N pH sensor mutants were measured using ramp protocols and standard extracellular divalent-free solutions (adjusted to pH 6.0 and 8.5 with HCl and NaOH, respectively) as described previously (23). Online alterations in extracellular pH were achieved by perfusion of the extracellular solution surrounding the clamped cell.

Functional recovery after chemobleaching. MDCK-EGFP-TRPV5 cells were incubated for 10 min with 5 mM 2-(trimethylammonium)ethyl methanethiosulfonate bromide (MTSET) in KHB, pH 7.4, to nullify all TRPV5 channels on the cell surface. Cells were washed three times with KHB, pH 7.4, before preincubation for 10 min in KHB, pH 6.0, pH 7.4, or pH 8.5, and subsequent $^{45}Ca^{2+}$ uptake to investigate the recovery of TRPV5 channels on the functional level. Total block was investigated by adding 5 mM MTSET to all buffers, and 10 μM ruthenium red was added to investigate ruthenium red sensitivity of the functional recovery. In another approach, pCINEO/IRES-EGFP-TRPV5 transiently transfected HEK293 cells were incubated for 10 min with 5 mM MTSET in standard extracellular divalent-free solution before starting patch clamp measurements. The recovery after chemobleaching was determined in divalent-free extracellular solutions of pH 6.0, pH 7.4, or pH 8.5. A total block of the current was established by including 5 mM MTSET in all extracellular solutions.

Confocal microscopy, TIRF microscopy, and image analysis. Live-cell confocal images were taken using a Zeiss LSM510meta microscope (Carl Zeiss GmbH, Jena, Germany) with a PlanApochromatic 63× 1.4 oil immersion differential interference-contrast lens (Carl Zeiss GmbH) at room temperature. A custom-built objective-based TIRF microscope, as described in detail previously (2), was used to image EGFP-labeled proteins in close proximity to the cell surface. Cells grown on glass coverslips were placed in a custom-made chamber with a standard external solution (135 mM NaCl, 5 mM KCl, 1.5 mM $MgCl_2$, 1.5 mM $CaCl_2$, 20 mM HEPES, 10 mM D-glucose, pH 6.0 or pH 8.5, with HCl/NaOH) and imaged at room temperature. Cells were analyzed for 100 s (one frame per second) at pH 6.0 to establish a baseline in whole-cell TIRF measurements before switching to pH 8.5 by whole-bath perfusion. After 150 s, extracellular pH was reduced to pH 6.0 and images were taken for 150 s. To quantify changes in TIRF, intensities of the regions of interests of several (n = 5 to 6) cells, with areas between 5 to 10% of the footprint of the cell, were averaged and normalized according to the following equation: relative change = $I(t) - I(0)$, where $I(0)$ is the intensity at the beginning of the time series and $I(t)$ is the intensity at time point t. Changes in the mean square displacement (MSD) and diffusion constant (D) were calculated as described previously (19).

Biotinylation. HEK293T cells were transfected with pCINEO/IRES-GFP-HA-TRPV5 or pCINEO/IRES-GFP. Cells were incubated at 37°C with standard external solution, pH 6.0 or pH 8.5, for 10 min before cells were placed on ice to inhibit endo- and exocytosis. Biotinylation was performed on ice, and cells were lysed as described previously (4). Thus, at the point of biotin incubation, the pH of the solutions was equal in all conditions, thereby preventing differences in cell surface labeling due to pH sensitivity of biotinylation. Subsequently, cell surface proteins were precipitated with neutravidin-agarose beads. The purified biotinylated surface proteins were probed for the presence of TRPV5 by immunoblotting using anti-TRPV5.

Statistical analysis. In all experiments, data are expressed as means ± standard errors of the means. Overall statistical significance was determined by analysis of variance, followed by Bonferroni contrast analysis to investigate individual significance using Instat 3 software for Macintosh (San Diego, CA). P values below 0.05 were considered significant.

RESULTS

Extracellular pH determines TRPV5-mediated Ca^{2+} influx. In kidney, TRPV5 is exposed to prourine pH values ranging from 6 to 7 (10). Using electrophysiological recordings, TRPV5 has been reported to be regulated by both intra- and extracellular pH (25, 26). To further assess the role of extracellular pH in TRPV5 activity, $^{45}Ca^{2+}$ uptake in transiently transfected HEK293T cells was determined at different extracellular pH values. At pH 6.0, $^{45}Ca^{2+}$ uptake of TRPV5-expressing cells was not significantly different from that of mock (EGFP)-transfected cells, indicating a lack of functional TRPV5 channels at the cell surface. At pH 7.4, however, $^{45}Ca^{2+}$ uptake of TRPV5-expressing cells was significantly higher than that of mock-transfected cells and extracellular alkalinization (pH 8.5) further increased $^{45}Ca^{2+}$ uptake of TRPV5-expressing cells (Fig. 1A). Interestingly, extracellular pH had no significant effect on TRPM7-mediated $^{45}Ca^{2+}$ uptake in this pH range, showing the specificity of the pH effect on TRPV5 activity (Fig. 1B). Furthermore, electrophysiological recordings of HEK293 cells transiently expressing TRPV5 were used to investigate the pH dependence of channel activity. Extracellular alkalinization from pH 6.0 to 8.5 resulted in a rapid increase in TRPV5 currents, while extracellular acidification from pH 8.5 to pH 6.0 revealed a rapid decrease in TRPV5 currents (Fig. 1C).

The intracellular lysine (K607) and the extracellular glutamic acid (E522) residues of TRPV5 have been postulated as pH sensors regulating TRPV5 activity, although K607N and E522Q mutants still displayed pH sensitivity (25, 26). To further assess the pH dependence of these mutants, whole-cell patch clamp and $^{45}Ca^{2+}$ uptake measurements were performed with HEK293 cells transiently expressing these mutated channels. Cells expressing EGFP-TRPV5 E522Q or EGFP-TRPV5 K607N exhibited pH-dependent change in whole-cell currents (Fig. 1C) and $^{45}Ca^{2+}$ uptake activity, which was not significantly different from that of wild-type EGFP-TRPV5 (Fig. 1D). Importantly, the expression levels of these mutants were equal to that of wild-type EGFP-TRPV5 (Fig. 1E).

Extracellular alkalinization stimulates the insertion of TRPV5 at the plasma membrane. pH-dependent $^{45}Ca^{2+}$ uptake in TRPV5-expressing cells can be explained by altered activity of TRPV5 present at the cell surface or changes in the number of functional TRPV5 channels at the plasma membrane. Because cellular trafficking processes like endo- and exocytosis are regulated by extracellular pH (8, 12, 14), the trafficking of TRPV5 was assessed by TIRF microscopy. Detailed analysis of EGFP-labeled TRPV5 in transiently transfected HEK293T cells with live-cell confocal and TIRF microscopy revealed a highly motile punctuate distribution pattern with no clear plasma membrane localization (Fig. 2A and 3; see also Movies IA and IB at http://idisk.mac.com/r.bindels-Public/MCB_submission). Immunocytochemistry in fixed cells expressing TRPV5 showed no colocalization of the channel with markers for endosomes (EEA1), lipid rafts (caveolin-1), endoplasmic reticulum (58 kDa), and lysosomes (LAMP1) (data not shown). TIRF microscopy indicated that these EGFP-TRPV5-containing vesicles move in an undirected manner (see movie IB at the above URL). To

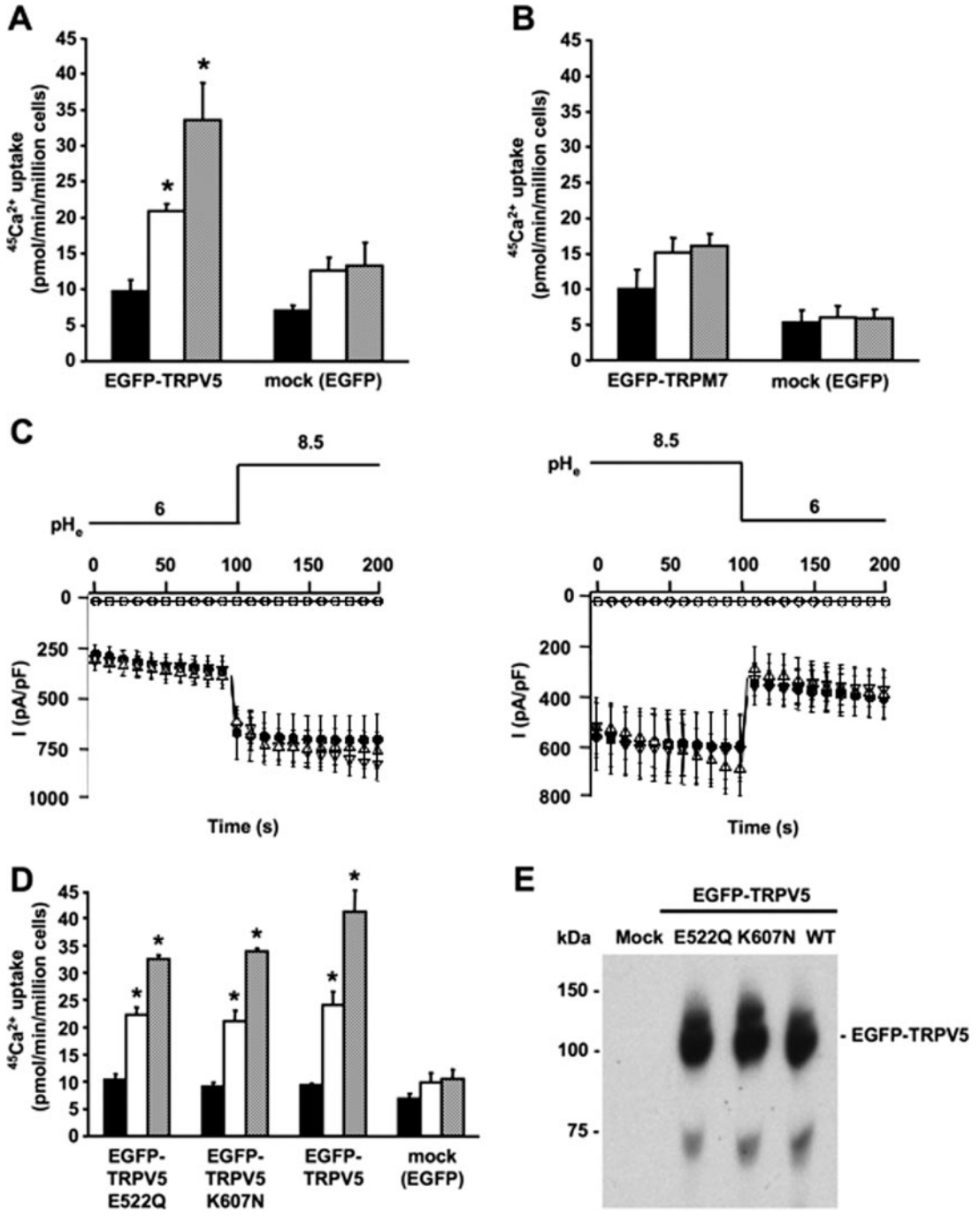

FIG. 1. Alkaline pH stimulates the activity of TRPV5. $^{45}Ca^{2+}$ uptake at different extracellular pH values for HEK293T cells expressing EGFP-TRPV5 ($n = 6$) (A) or EGFP-TRPM7 ($n = 6$) (B) compared to $^{45}Ca^{2+}$ uptake of mock (EGFP)-transfected cells ($n = 6$). $^{45}Ca^{2+}$ uptake is represented by black bars for pH 6.0, white bars for pH 7.4, and gray bars for pH 8.5. (C) Averaged whole-cell currents measured from 400-ms voltage ramps (interval = 10 s) in nominally divalent-free solution from HEK293 cells transiently expressing TRPV5 (●), TRPV5 E522Q (▽), or TRPV5 K607N (△) or mock-transfected cells (○) ($n = 10$ cells for each condition). Extracellular pH was switched at indicated time points. (D) Comparison of alkaline pH-stimulated $^{45}Ca^{2+}$ uptake in HEK293T cells transfected with EGFP, EGFP-TRPV5, EGFP-TRPV5 E522Q, or EGFP-TRPV5 K607N. $^{45}Ca^{2+}$ uptake is represented by black bars for pH 6.0, white bars for pH 7.4, and gray bars for pH 8.5. (E) Expression of EGFP-TRPV5 and EGFP-TRPV5 mutants as analyzed by immunoblotting using the anti-GFP antibody. Significant differences in pH-dependent $^{45}Ca^{2+}$ uptake compared to that for mock-transfected cells are indicated by an asterisk ($P < 0.05$).

investigate the influence of extracellular pH on these EGFP-TRPV5-containing vesicles, TIRF microscopy was applied to monitor the number and proximity of vesicles to the plasma membrane in response to changes in extracellular pH (Fig. 2B and C; also see Movie IIA at the above URL). Alkalinization resulted in a rapid elevation of the overall EGFP-TRPV5 TIRF signal to a peak plateau level, suggesting rapid recruitment and subsequent delivery of EGFP-

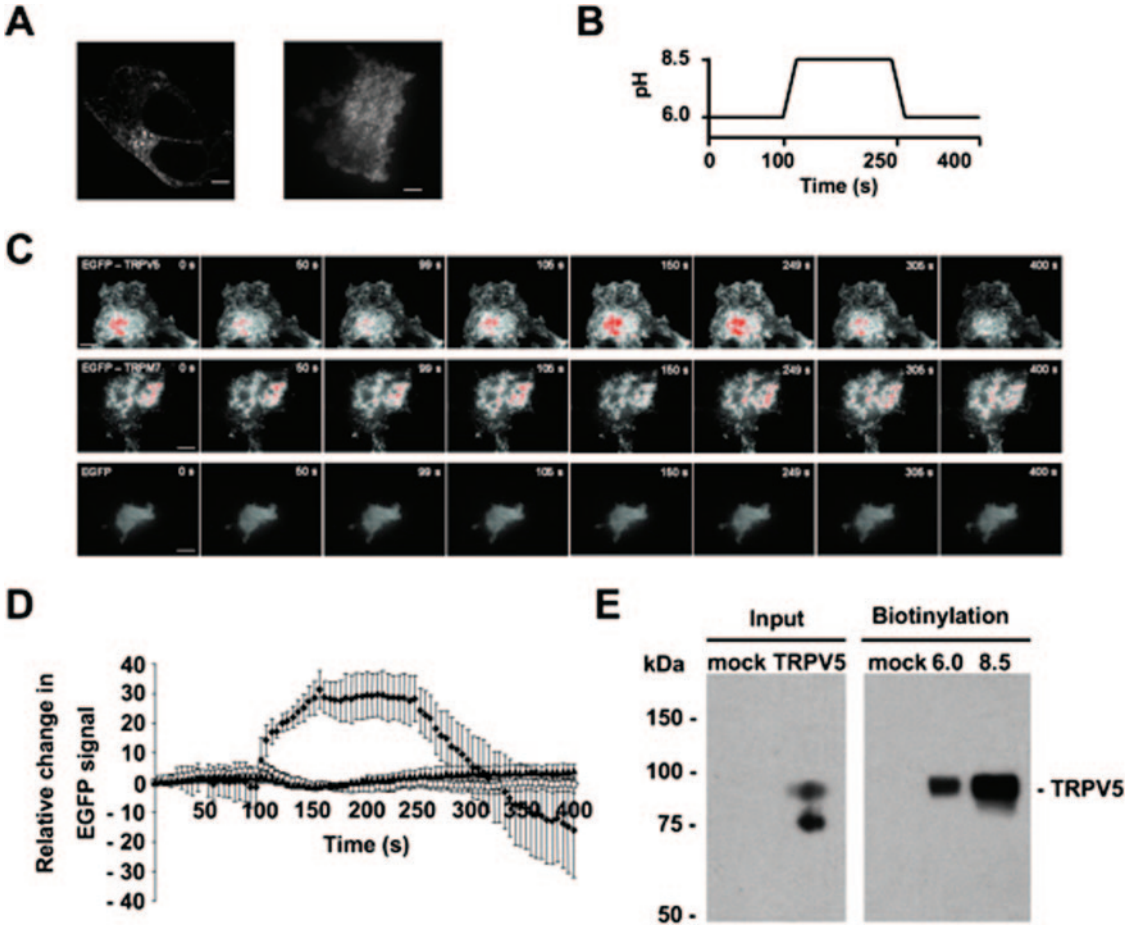

FIG. 2. Alkaline pH stimulates plasma membrane insertion of TRPV5 channels in HEK293T cells. (A) Confocal (left) and TIRF (right) image of a single HEK293T cell expressing EGFP-TRPV5 (see Movies IA and B at http://idisk.mac.com/r.bindels-Public/MCB_submission). Scale bar = 5 μm. (B and C) TIRF images of single HEK293T cells expressing EGFP-TRPV5, EGFP-TRPM7, or EGFP (see movies IIA, B, and C at the above URL). Scale bar = 10 μm. Cells were imaged as indicated in the figure, and extracellular pH was switched at the indicated time points. Gradient filters were applied such that saturating levels turn red. (D) Time course of the overall EGFP fluorescence signal in EGFP-TRPV5 (◆) (n = 5)-, EGFP-TRPM7 (□) (n = 5)-, or EGFP (▲) (n = 5)-expressing HEK293T cells. (E) Cell surface expression of TRPV5 at different extracellular pH values as measured by cell surface biotinylation of HA-TRPV5-expressing HEK293T cells. Analysis of total TRPV5 expression revealed a nonglycosylated form (lower band) and a complex glycosylated form (upper) that is the band accessible to extracellular biotin. A representative blot of three independent experiments is shown.

TRPV5 to the plasma membrane (Fig. 2C and D). Subsequent acidification decreased the overall EGFP-TRPV5 TIRF signal to even below the initial unstimulated level of fluorescence, suggesting the retrieval of TRPV5 from the plasma membrane to a cytosolic compartment. Importantly, no significant changes in TIRF signal were observed in EGFP-TRPM7- or EGFP-transfected HEK293T cells when switching the pH from 6.0 to 8.5 or from 8.5 to 6.0 (Fig. 2C and D; also see Movies IIB and C at the above URL). This indicates that the recruitment of TRPM7 is independent of extracellular pH and that fluorescent changes were not due to a pH sensitivity of EGFP. TIRF microscopy is a valuable method for studying protein movements within the periplasmic space. However, this technique cannot distinguish between surface expression and the presence of proteins just underneath the plasma membrane. Thus, the actual accessibility to the external environment cannot be determined using this technique. Therefore, cell surface biotinylation was applied to investigate the localization of TRPV5 in the plasma membrane at different extracellular pH values (Fig. 2E). Importantly, at the point of incubation with biotin, the pH of the solutions was equal in all conditions to prevent differences in cell surface labeling due to pH sensitivity of biotinylation (see Materials and Methods for details). In line with the results obtained with TIRF microscopy, cell surface expression of TRPV5 was significantly increased (2.35-fold ± 0.75-fold) at pH 8.5 compared to that at pH 6.0.

Functional recovery after chemobleaching of TRPV5 activity is regulated by extracellular pH. MDCK cells stably expressing TRPV5 were used to assess the pH dependence of TRPV5 trafficking by FRAC (20). MDCK cells are convenient for imaging EGFP-TRPV5-containing vesicles in contrast to transfected HEK293T cells that display a high density of EGFP-TRPV5-containing vesicles (Fig. 3). In agreement with the results observed with HEK293T cells, extracellular alkalinization of TRPV5-expressing MDCK cells resulted in rapid re-

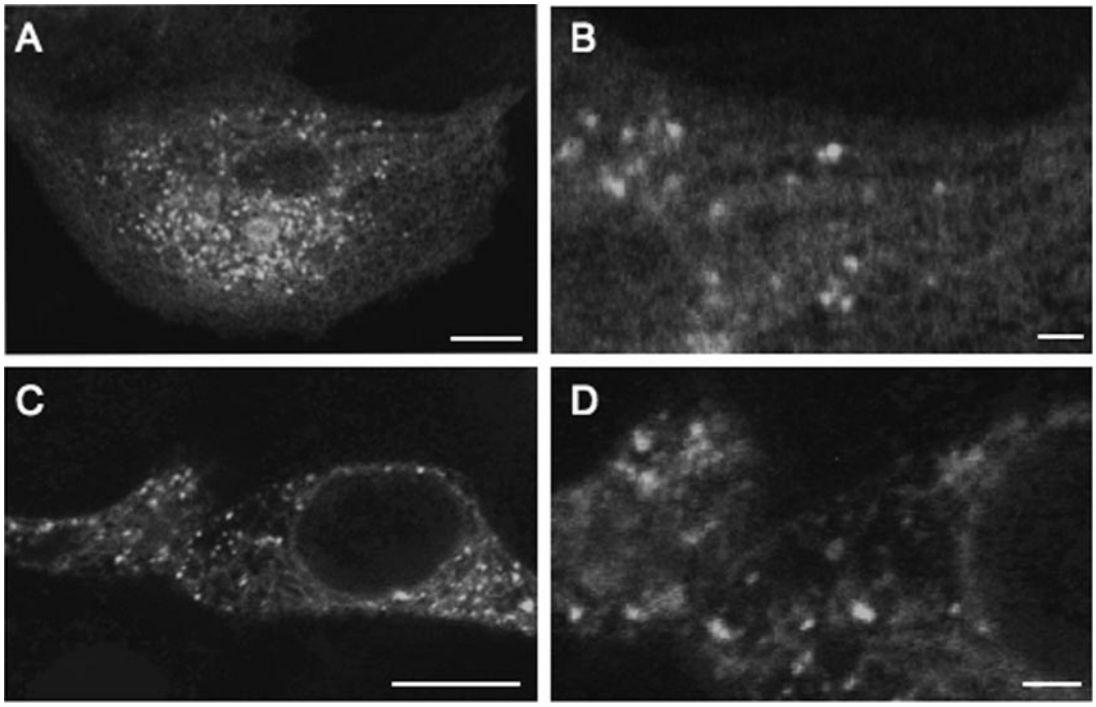

FIG. 3. Confocal images of TRPV5 expressing HEK293T and MDCK cells. Confocal image of a single (A) and a magnified (B) MDCK cell stably expressing EGFP-TRPV5 and a single (C) and a magnified (D) HEK293T cell transiently expressing EGFP-TRPV5. The scale bar in panels A and C indicates 10 μm and that in panels B and D indicates 2 μm.

cruitment of EGFP-TRPV5 towards the plasma membrane, while subsequent acidification reduced cell surface EGFP-TRPV5 expression (Fig. 4; also see Movie IIIA at the above URL). MTSET irreversibly binds to an accessible cysteine in the channel pore of wild-type rabbit TRPV5 (6). This enabled us to study FRAC without introducing cysteine residues in the TRPV5 pore, which could potentially alter intrinsic channel activity. The addition of MTSET to stably EGFP-TRPV5-expressing MDCK cells completely silenced $^{45}Ca^{2+}$ uptake at pH 6.0, 7.4, and 8.5 (Fig. 5A), confirming the accessibility of the cysteine in the TRPV5 pore and the blockade by MTSET. Cells preincubated for only 10 min with MTSET showed a subsequent functional recovery of $^{45}Ca^{2+}$ uptake at pH 7.4 and 8.5, whereas no recovery was observed at pH 6.0. At pH 8.5, the recovery of $^{45}Ca^{2+}$ uptake was significantly increased compared to the recovery at pH 7.4, demonstrating that extracellular alkalinization amplified the insertion of active TRPV5 channels. Furthermore, incubation with the TRPV5 channel antagonist ruthenium red (10 μM) during the $^{45}Ca^{2+}$ uptake completely inhibited functional recovery after MTSET treatment, indicating that the recovery is mediated by TRPV5. Moreover, the patch clamp technique was used to address the effect of extracellular pH on the recovery of TRPV5 whole-cell currents after chemobleaching with MTSET. After preincubation for 10 min with 5 mM MTSET, the recovery of TRPV5-mediated currents was significantly increased at pH 8.5 compared to that at pH 7.4 (Fig. 5B). Continuous application of 5 mM MTSET abolished TRPV5-mediated currents at all pH values tested.

"Kiss and linger" plasma membrane delivery of TRPV5-containing vesicles. In MDCK cells stably expressing EGFP-TRPV5 TIRF, single-vesicle fluorescence rapidly increased after switching from pH 6.0 to 8.5 and reached a peak plateau level within 10 to 20 s, whereas subsequent extracellular acidification decreased the vesicle fluorescence (Fig. 6A and B; also see Movie IIIB at the above URL). These findings indicate that recruitment to and subsequent retrieval of single TRPV5-containing vesicles from the plasma membrane are affected by extracellular pH. Moreover, TRPV5-containing vesicles appeared to fuse with the plasma membrane interface, but did not collapse since the fluorescence intensity did not disperse after reaching the peak plateau level. In addition, the number of vesicles within the TIRF field did not increase, suggesting that the rise in fluorescence reflects the rapid recruitment of TRPV5-containing vesicles just underneath the plasma membrane.

To determine the vesicle motility upon consecutively extracellular alkalinization and acidification, we calculated the MSD (Fig. 6C). Upon extracellular alkalinization TRPV5-containing vesicles were rapidly converted in lateral motility from a high to a more restricted velocity. The decrease in MSD occurred as the vesicle fluorescence increased, suggesting the capture of TRPV5-containing vesicles at the plasma membrane as soon as they approach the cell surface. During subsequent decrease of vesicle fluorescence due to extracellular acidification, TRPV5-containing vesicles are rapidly converted to a high lateral motility, suggesting retrieval from the plasma membrane to a cytosolic compartment. Note that the average diffusion constants, as calculated from changes in MSD (19) of several vesicles from different cells before recruitment and after retrieval, were identical (Fig. 6D). Because the diffusion constant is deter-

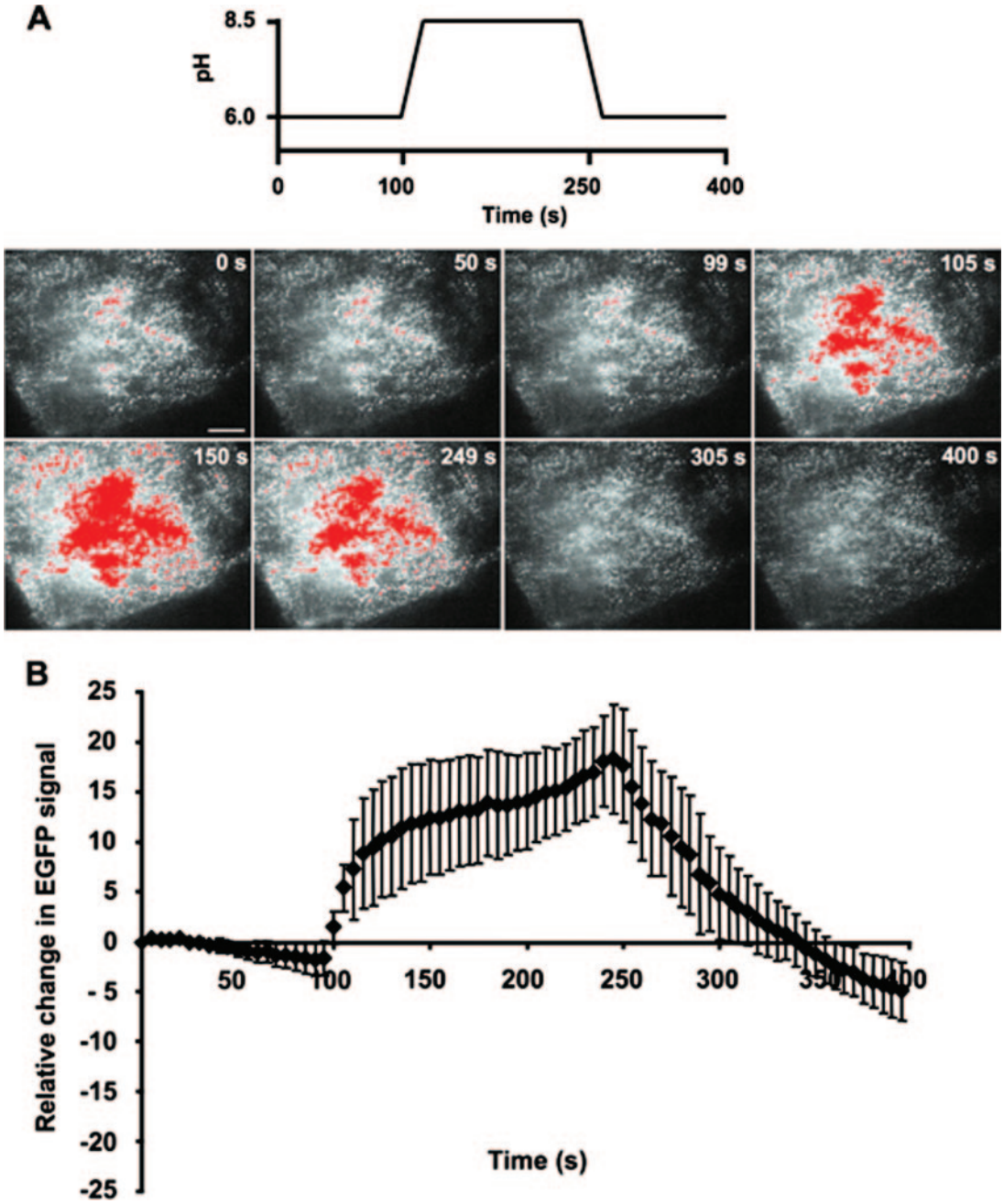

FIG. 4. Plasma membrane recruitment of EGFP-TRPV5 in MDCK cells upon extracellular alkalinization. (A) TIRF microscopy images of a single MDCK cell stably expressing EGFP-TRPV5. Cells were imaged as indicated in the figure, and extracellular pH was switched at indicated time points (see Movie IIIA [http://idisk.mac.com/r.bindels-Public/MCB_submission]). Scale bar = 10 μm. (B) Time course of the overall EGFP fluorescence signal in EGFP-TRPV5-expressing MDCK cells (n = 6).

mined by the radius of the vesicle as reflected by the Stokes and Einstein equation (18), these findings further support that TRPV5-containing vesicles remain intact during the delivery of TRPV5 to the cell surface.

DISCUSSION

The present study identifies extracellular pH as a dynamic switch controlling TRPV5 cell surface expression and, thereby, TRPV5 activity. This conclusion is based on the following experimental observations. (i) Extracellular alkalinization increases, whereas acidification decreases TRPV5 channel activity. (ii) Extracellular alkalinization induces rapid recruitment of EGFP-TRPV5-containing vesicles, which fuse but do not collapse into the plasma membrane interface, whereas subsequent acidification results in the retrieval of TRPV5-containing vesicles. (iii) Extracellular alkalinization augments the number of TRPV5 channels at the plasma membrane as ana-

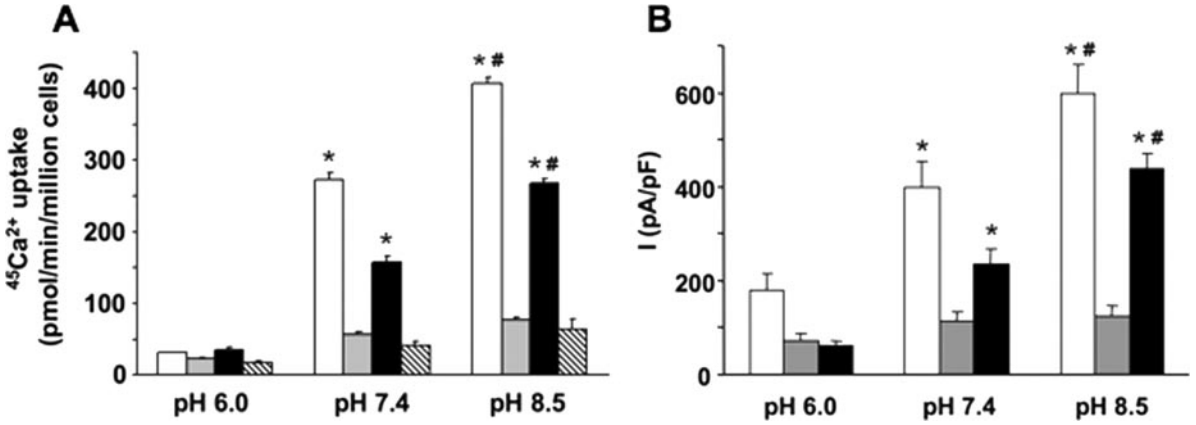

FIG. 5. Functional recovery of TRPV5 activity after chemobleaching is elevated at alkaline pH. (A) $^{45}Ca^{2+}$ uptake at different extracellular pH values of MDCK cells stably expressing EGFP-TRPV5 ($n = 6$). To inhibit TRPV5-mediated $^{45}Ca^{2+}$ uptake, 10 μM of ruthenium red was added. The irreversible blocker MTSET (5 mM) was applied to study the functional recovery of TRPV5 after MTSET treatment. White bars represent $^{45}Ca^{2+}$ uptake under normal conditions, gray bars represent the continuous presence of MTSET, black bars represent recovery after MTSET treatment, and hatched bars represent recovery in the presence of ruthenium red. Significant differences in pH-dependent $^{45}Ca^{2+}$ uptake compared to that in MTSET- or ruthenium red-treated cells are indicated by an asterisk ($P < 0.05$). Significant increases in $^{45}Ca^{2+}$ uptake compared to $^{45}Ca^{2+}$ uptake at pH 7.4 are indicated by a number symbol ($P < 0.05$). (B) After 10 min of MTSET pretreatment, whole-cell currents recorded from HEK293 cells transiently transfected with TRPV5 were measured in extracellular solution at the specified pH ($n = 8$). White bars represent the average current densities in the absence of MTSET, gray bars indicate the average current densities with MTSET continuously present in the extracellular solution, and black bars show the recovered currents after MTSET pretreatment. Asterisks indicate a significant difference ($P < 0.05$) compared to that for cells continuously treated with MTSET and the number symbol shows a significant difference ($P < 0.05$) compared to the average current measured in normal extracellular solution (without MTSET) at pH 7.4.

lyzed by cell surface protein biotinylation. (iv) Functional recovery of TRPV5 activity after chemobleaching is dependent on extracellular pH. (v) TRPV5 vesicles undergo a rapid conversion in lateral motility from high to restricted as they approach the membrane and vice versa during manipulation of the extracellular pH.

Here, we showed that the activity of TRPV5 is directly controlled by the extracellular pH as measured by electrophysiological recordings and $^{45}Ca^{2+}$ uptake analysis. This is in line with our previous studies demonstrating that the current density of TRPV5-expressing HEK293 cells is significantly smaller at pH 6.0 than at pH 7.4. At pH 8.5, they were slightly larger (24–26). Subsequently, Huang and coworkers further substantiated our findings by showing that both extracellular and intracellular acidification reduce intrinsic TRPV5 channel activity (24–26). In addition, two pH-sensing residues were identified in TRPV5. Compared to wild-type TRPV5, the mutation of these amino acids (K607N and E522Q) revealed a significantly diminished electrophysiological response to intra- and extracellular pH, although the overall pH sensitivity persisted. Our $^{45}Ca^{2+}$ uptake and patch clamp experiments indicated that the mutation of these residues does not change the activity of TRPV5 in the pH range of 6.0 to 8.5, suggesting that the role of these amino acids as pH sensors is less pronounced than previously assumed. Despite this apparent controversy, all observations show an important physiological role of extracellular pH in determining TRPV5 activity. Indeed, the pH of the prourine in the TRPV5-expressing tubule segments normally varies between 6 and 7, a range by which TRPV5 activity is significantly altered. Furthermore, early observations showed that urinary Ca^{2+} excretion increases during metabolic and respiratory acidosis (3, 21), which is in line with the observed pH sensitivity of TRPV5.

To determine the molecular mechanism by which extracellular protons inhibit TRPV5 channel activity, a comprehensive set of experiments was performed. Together, TIRF analysis, biotinylation assays, and functional recovery of TRPV5 activity after chemobleaching demonstrated that extracellular pH determines the cell surface localization of TRPV5. Importantly, the increase in single-vesicle recruitment upon alkalinization was accompanied by a rise in TRPV5 activity, suggesting capture of functional channels at the plasma membrane. Subsequent acidification decreased the TRPV5 activity that was accompanied by retrieval of TRPV5-containing vesicles from the plasma membrane to the cytosol. The observed difference in time course between TIRF whole-cell fluorescence and TRPV5 activity measured by electrophysiology could be due to the relocation of a particular group of fluorescent structures towards the plasma membrane that do not fuse. Previous data describing that conformational changes within the channel pore are coupled to the inhibition of TRPV5 by protons (25), together with our results, suggest that the extracellular pH affects the activity of TRPV5 via multiple mechanisms. Both TRPV5 trafficking to and activity at the cell surface are inhibited by extracellular protons, indicating an efficient regulation of TRPV5 activity during changes in extracellular pH.

TIRF analysis revealed that upon stimulation by extracellular alkalinization, the EGFP-TRPV5 fluorescence of single vesicles rapidly reaches a peak plateau level. Importantly, this fluorescence signal did not subsequently disperse, while the pH was maintained at 8.5, suggesting that the TRPV5-containing vesicles are not collapsed into the plasma membrane, but rather remain intact at the membrane interface. This finding is different from that observed with TIRF recordings of GLUT4-containing vesicles or synaptic vesicles (9, 13). Upon stimulation, GLUT4-containing vesicles were recruited towards the

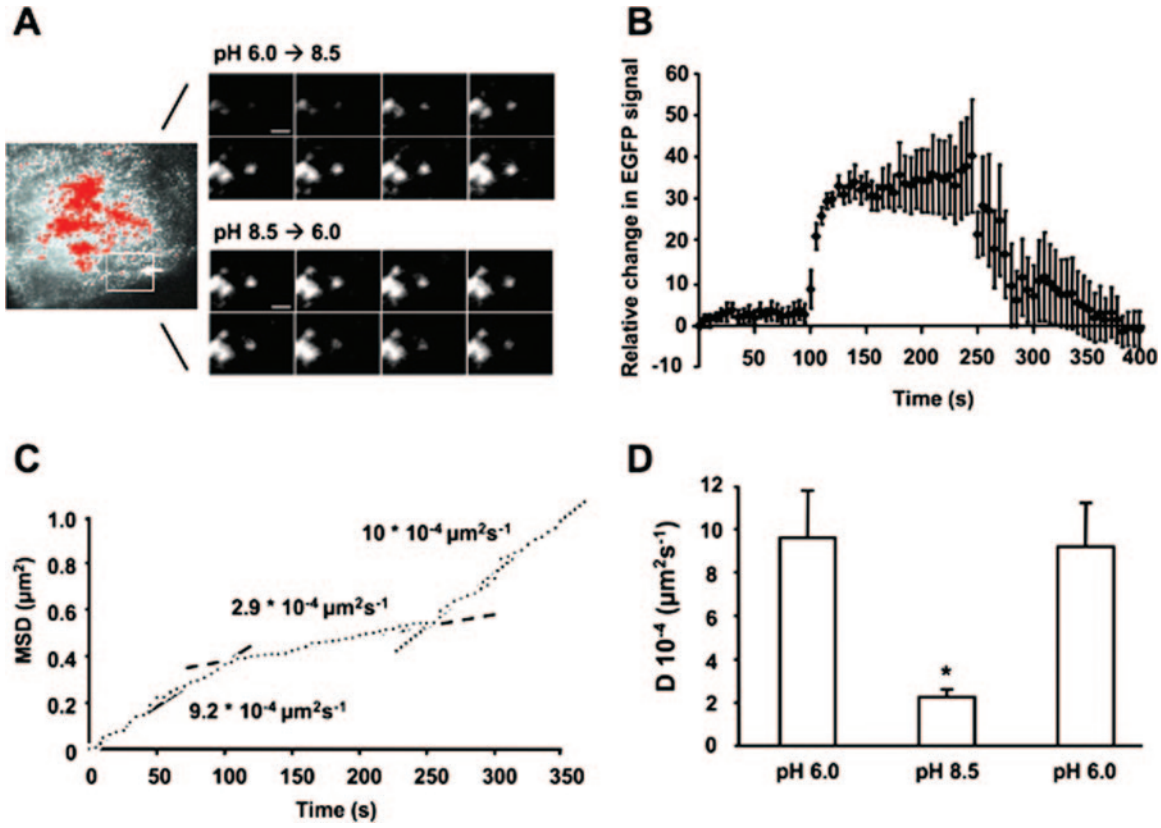

FIG. 6. Alkaline pH stimulates plasma membrane recruitment of TRPV5-containing vesicles in MDCK cells. (A) TIRF images of a single vesicle in MDCK cells stably expressing EGFP-TRPV5 directly after extracellular alkalinization (upper panel) and subsequent acidification (lower panel) (see Movie IIIB [http://idisk.mac.com/r.bindels-Public/MCB_submission]). Time interval between images is 3 s. Scale bar = 2 μm. (B) Average time course of single-vesicle fluorescence in EGFP-TRPV5-expressing MDCK cells (n = 5). (C) The mean square displacement (plotted accumulative in time) of the vesicle shown in panel A reveals a rapid conversion from cytosolic diffusion at pH 6.0 (solid line) to a more restricted lateral motion at pH 8.5 (dashed line) and back to free cytosolic diffusion at pH 6.0 (dotted line). (D) Averaged vesicle diffusion constant (n = 10 vesicles) during the protocol (pH 6.0 at time points 0 to 100 s, pH 8.5 at 125 to 250 s, and a subsequent pH 6.0 at 275 to 400 s). A significant difference in the diffusion constant compared with cells exposed to pH 6.0 is indicated by an asterisk ($P < 0.05$).

cell surface where they completely collapsed into the membrane and GLUT4 diffused into the plasma membrane as reflected by the dispersion of the vesicle fluorescence. On the other hand, synaptic vesicles translocated towards the plasma membrane after stimulation where a transient opening with the plasma membrane is formed. Upon exocytosis of its cargo, these vesicles immediately relocated to the cytosol as measured by the sudden loss in fluorescence of intact vesicles (termed "kiss and run") (7). TRPV5 recruitment during extracellular alkalinization is, however, comparable with plasma membrane recruitment of TRPC5-containing vesicles by EGF stimulation (2). After the initiation of plasma membrane recruitment, TRPV5- and TRPC5-containing vesicles did not fully collapse into the membrane as reflected by the lack of fluorescence diffusion and disappearance of single vesicles after reaching the cell surface. These channels might access the extracellular solution from inside the vesicle membrane (referred to as "kiss and linger"), as supported by the accompanied increase in activity, enhanced accessibility to biotin and, for TRPV5, increased FRAC. Because several TRP channels, including TRPV5 and TRPC5, display constitutive activity, the suggested "kiss and linger" mechanism of channel delivery to the plasma membrane is attractive since this novel concept integrates a direct response to physiological stimuli by TRP channel insertion. The experiments with TRPC5 could not distinguish between the collapsing of vesicles and the subsequent diffusion of the channel into the plasma membrane or transient interaction of the vesicles with the plasma membrane (2). The performed experiments, however, enabled us to control TRPV5 plasma membrane expression by consecutive alkalinization and acidification of the extracellular solution. Our results indicate that single vesicles, located just underneath the plasma membrane, are rapidly recruited towards the plasma membrane upon extracellular alkalinization, linger at the plasma membrane without collapsing, and are subsequently retrieved to the cytosol upon removal of the stimulus (i.e., extracellular acidification). Together with the increase in TRPV5 activity, enhanced accessibility to biotin, and functional recovery of TRPV5 activity after chemobleaching, this suggests that upon extracellular alkalinization, recruited TRPV5 accesses the extracellular environment via transient openings because the same vesicles are relocated intact upon extracellular acidification. Comparable with secretory vesicles in synapses, vesicles are recaptured largely intact after exocytosis (7, 22). Thus, recapturing nonfused vesicles from the plasma membrane might occur via uniform mechanisms.

In summary, these findings demonstrate recruitment of TRPV5 to the cell surface as a novel mechanism underlying pH-sensitive, TRPV5-mediated Ca^{2+} transport. They also contribute to the concept that activation of constitutive active ion channels relies on "kiss and lingering" vesicles which fuse but do not collapse during the process of plasma membrane recruitment and subsequent retrieval.

ACKNOWLEDGMENTS

This work was supported by the Dutch Organization of Scientific Research (Zon-M_w 016.006.001, NWO-ALW 805.09.042), Human Frontiers Science Program (RGP32/2004), the European Science Foundation (EURYI), and the Dutch Kidney Foundation (C03.6017) and a grant of the van Walree Fund from the Royal Dutch Academy of Sciences to support the work visit of T. T. Lambers to the lab of D. Clapham.

REFERENCES

1. **Bähner, M., S. Frechter, N. Da Silva, B. Minke, R. Paulsen, and A. Huber.** 2002. Light-regulated subcellular translocation of *Drosophila* TRPL channels induces long-term adaptation and modifies the light-induced current. Neuron **34:**83–93.
2. **Bezzerides, V. J., I. S. Ramsey, S. Kotecha, A. Greka, and D. E. Clapham.** 2004. Rapid vesicular translocation and insertion of TRP channels. Nat. Cell Biol. **6:**709–720.
3. **Canzanello, V. J., M. Bodvarsson, J. A. Kraut, C. A. Johns, E. Slatopolsky, and N. E. Madias.** 1990. Effect of chronic respiratory acidosis on urinary calcium excretion in the dog. Kidney Int. **38:**409–416.
4. **Chang, Q., S. Hoefs, A. W. van der Kemp, C. N. Topala, R. J. Bindels, and J. G. Hoenderop.** 2005. The beta-glucuronidase klotho hydrolyzes and activates the TRPV5 channel. Science **310:**490–493.
5. **den Dekker, E., J. Schoeber, C. N. Topala, S. F. van de Graaf, J. G. Hoenderop, and R. J. Bindels.** 2005. Characterization of a Madin-Darby canine kidney cell line stably expressing TRPV5. Pflueg. Arch. **450:**236–244.
6. **Dodier, Y., U. Banderali, H. Klein, O. Topalak, O. Dafi, M. Simoes, G. Bernatchez, R. Sauve, and L. Parent.** 2004. Outer pore topology of the ECaC-TRPV5 channel by cysteine scan mutagenesis. J. Biol. Chem. **279:** 6853–6862.
7. **Gandhi, S. P., and C. F. Stevens.** 2003. Three modes of synaptic vesicular recycling revealed by single-vesicle imaging. Nature **423:**607–613.
8. **Glunde, K., S. E. Guggino, M. Solaiyappan, A. P. Pathak, Y. Ichikawa, and Z. M. Bhujwalla.** 2003. Extracellular acidification alters lysosomal trafficking in human breast cancer cells. Neoplasia **5:**533–545.
9. **Gundelfinger, E. D., M. M. Kessels, and B. Qualmann.** 2003. Temporal and spatial coordination of exocytosis and endocytosis. Nat. Rev. Mol. Cell Biol. **4:**127–139.
10. **Hoenderop, J. G., B. Nilius, and R. J. Bindels.** 2005. Calcium absorption across epithelia. Physiol. Rev. **85:**373–422.
11. **Kanzaki, M., Y. Q. Zhang, H. Mashima, L. Li, H. Shibata, and I. Kojima.** 1999. Translocation of a calcium-permeable cation channel induced by insulin-like growth factor-I. Nat. Cell Biol. **1:**165–170.
12. **Keyes, S. R., and G. Rudnick.** 1982. Coupling of transmembrane proton gradients to platelet serotonin transport. J. Biol. Chem. **257:**1172–1176.
13. **Li, C. H., L. Bai, D. D. Li, S. Xia, and T. Xu.** 2004. Dynamic tracking and mobility analysis of single GLUT4 storage vesicle in live 3T3-L1 cells. Cell Res. **14:**480–486.
14. **Lindgren, C. A., D. G. Emery, and P. G. Haydon.** 1997. Intracellular acidification reversibly reduces endocytosis at the neuromuscular junction. J. Neurosci. **17:**3074–3084.
15. **Montell, C., L. Birnbaumer, V. Flockerzi, R. J. Bindels, E. A. Bruford, M. J. Caterina, D. E. Clapham, C. Harteneck, S. Heller, D. Julius, I. Kojima, Y. Mori, R. Penner, D. Prawitt, A. M. Scharenberg, G. Schultz, N. Shimizu, and M. X. Zhu.** 2002. A unified nomenclature for the superfamily of TRP cation channels. Mol. Cell **9:**229–231.
16. **Nijenhuis, T., K. Y. Renkema, J. G. Hoenderop, and R. J. Bindels.** 2006. Acid-base status determines the renal expression of Ca^{2+} and Mg^{2+} transport proteins. J. Am. Soc. Nephrol. **17:**617–626.
17. **Oancea, E., J. T. Wolfe, and D. E. Clapham.** 2006. Functional TRPM7 channels accumulate at the plasma membrane in response to fluid flow. Circ. Res. **98:**245–253.
18. **Rusakov, D. A., and D. M. Kullmann.** 1998. Geometric and viscous components of the tortuosity of the extracellular space in the brain. Proc. Natl. Acad. Sci. USA **95:**8975–8980.
19. **Steyer, J. A., and W. Almers.** 1999. Tracking single secretory granules in live chromaffin cells by evanescent-field fluorescence microscopy. Biophys. J. **76:**2262–2271.
20. **Sun, H., S. Shikano, Q. Xiong, and M. Li.** 2004. Function recovery after chemobleaching (FRAC): evidence for activity silent membrane receptors on cell surface. Proc. Natl. Acad. Sci. USA **101:**16964–16969.
21. **Sutton, R. A., N. L. Wong, and J. H. Dirks.** 1979. Effects of metabolic acidosis and alkalosis on sodium and calcium transport in the dog kidney. Kidney Int. **15:**520–533.
22. **Taraska, J. W., D. Perrais, M. Ohara-Imaizumi, S. Nagamatsu, and W. Almers.** 2003. Secretory granules are recaptured largely intact after stimulated exocytosis in cultured endocrine cells. Proc. Natl. Acad. Sci. USA **100:**2070–2075.
23. **van de Graaf, S. F., J. G. Hoenderop, D. Gkika, D. Lamers, J. Prenen, U. Rescher, V. Gerke, O. Staub, B. Nilius, and R. J. Bindels.** 2003. Functional expression of the epithelial Ca^{2+} channels (TRPV5 and TRPV6) requires association of the S100A10-annexin 2 complex. EMBO J. **22:**1478–1487.
24. **Vennekens, R., J. Prenen, J. G. Hoenderop, R. J. Bindels, G. Droogmans, and B. Nilius.** 2001. Modulation of the epithelial Ca^{2+} channel ECaC by extracellular pH. Pflueg. Arch. **442:**237–242.
25. **Yeh, B. I., Y. K. Kim, W. Jabbar, and C. L. Huang.** 2005. Conformational changes of pore helix coupled to gating of TRPV5 by protons. EMBO J. **24:**3224–3234.
26. **Yeh, B. I., T. J. Sun, J. Z. Lee, H. H. Chen, and C. L. Huang.** 2003. Mechanism and molecular determinant for regulation of rabbit transient receptor potential type 5 (TRPV5) channel by extracellular pH. J. Biol. Chem. **278:**51044–51052.